Geomechanics and Engineering, Vol. 5, No. 1 (2013) 71-86
DOI: http://dx.doi.org/10.12989/gae.2013.5.1.071

Strength characteristics of transversely isotropic rock materials

Xue-Qiang Yang*, Li-Juan Zhang and Xiao-Ming Ji

Civil and Traffic Engineering School, Guangdong University of Technology, Guangzhou, 510090, China

(Received July 31, 2012, Revised December 30, 2012, Accepted January 10, 2013)

Abstract. For rock materials, a transversely isotropic failure criterion established through the extended Lade-Duncan failure criterion incorporating an anisotropic state scalar parameter, which is a joint invariant of deviatoric microstructure fabric tensor and normalized deviatoric stress tensor, is verified with the results of triaxial compressive data on Tournemire shale. For torsional shear mode with $0 \leq b \leq 0.75$, rock shear strengths decrease with α increasing until the rock shear strength approaches minimum value at $\alpha \approx 40°$, and after this point, the rock shear strengths increase as α increases further. For the torsional shear mode with $b > 0.75$, rock shear strengths are almost constant for $\alpha \leq 40°$, but it increases with increase in α afterwards. The rock shear strength variation against α agrees with shear strength changing tendency of heavily OCR natural London Clays tested before. Prediction results show that the transversely isotropic failure criterion proposed in the paper is reasonable.

Keywords: fabric tensor; transversely isotropy; anisotropic state scalar parameter; failure criterion

1. Introduction

The sedimentary consolidated clays, sands, and rocks in nature, exhibit strong inherent anisotropy, which is manifested as a directional dependence of deformation and strength characteristics. The anisotropy of these geomaterials is strongly related to their microstructure called fabric, in particular the existence of grain arrangement, crack pattern, bedding, foliation, etc. These materials are often encountered in foundations of a broad range of civil structures, in underground excavations, highways, as well as tunnels.

Over the last few decades, experimental studies, including sands (Oda 1972, Ochiai and Lade 1983), clay (Nishimara *et al.* 2007), and shale (Niandou *et al.* 1997), show that geomaterials present different failure strengths depending on the load orientation relative to their material principal axes. In the past, most geomaterial failure criteria were proposed based on a homogeneous media; therefore, an extended failure criterion incorporating material fabric tensor, inevitably has important theoretical and practical values.

Recently, an anisotropy state scalar parameter, which is a joint invariant of deviatoric microstructure fabric tensor and normalized deviatoric stress tensor, was proposed by Pietruszczak and Mroz (2001), Li *et al.* (2002), and Dafalias *et al.* (2004) respectively. Traditional isotropic constitutive model incorporating the anisotropy state scalar parameter, which has been proven to be a correct developing direction to deal with deformation and strength characteristics of natural

*Corresponding author, Professor, E-mail: xqyfls@126.com

structured geomaterials, makes it possible for further developing the failure criterion for transversely isotropic materials with a relatively simple expression form.

In this paper, first of all, a transversely isotropic failure criterion, established through the extended Lade-Duncan failure criterion (Yang *et al.* 2006a) incorporating the anisotropic state scalar parameter, is verified against Tournemire shale triaxial compressive testing data. Secondly, Tournemire shale strength characteristics on meridian and π planes, with different relative orientation between stress tensor and fabric tensor and with different stress level, is then revealed and discussed in detail, and these research results are further compared with data of heavily OCR natural London Clays published before. Finally, conclusion remarks are given.

2. Isotropic failure criterion of rock material

2.1 Lade-Duncan failure criterion

The sign of a stress component is taken to be positive for compression, and stress appearing in the article is meant to be effective stress. Under general stress states, some invariants of the stress tensor are expressed as

$$I_1 = \sigma_{ii} \tag{1}$$

$$I_2 = \sigma_{ij}\sigma_{ij} / 2 \tag{2}$$

$$I_3 = \sigma_{ij}\sigma_{jm}\sigma_{mi} / 3 \tag{3}$$

$$J_2 = s_{ij}s_{ij} / 2 \tag{4}$$

$$J_3 = s_{ij}s_{jm}s_{mi} / 3 \tag{5}$$

in which I_1, I_2 and I_3 are the first, second and third invariants of the stress tensor, respectively. J_2 and J_3 are the second and third invariants of the deviatoric stress tensor, and s_{ij} is deviatoric stress tensor with $s_{ij} = \sigma_{ij} - I_1\delta_{ij} / 3$, where δ_{ij} is a Kronecter symbol.

Lode angle θ_σ relating to J_2 and J_3, is written as

$$\theta_\sigma = \frac{1}{3}\sin^{-1}(-\frac{3\sqrt{3}}{2}\frac{J_3}{J_2^{3/2}}), \quad -\frac{\pi}{6} \le \theta_\sigma \le \frac{\pi}{6} \tag{6}$$

Lade and Duncan (1975) proposed the following failure criterion for sands

$$I_1^3 / I_3 = k_1 \tag{7}$$

in which k_1 is a parameter of the material.

Making $B = \sqrt{(k_1 - 27)/k_1}$, an alternative expression (Yang *et al.* 2006b) of Eq. (7) is

$$\sqrt{J_2} = \frac{BI_1}{2\sqrt{3}} g(\theta_\sigma) \tag{8}$$

where $g(\theta_\sigma)$ is an interpolating function written as

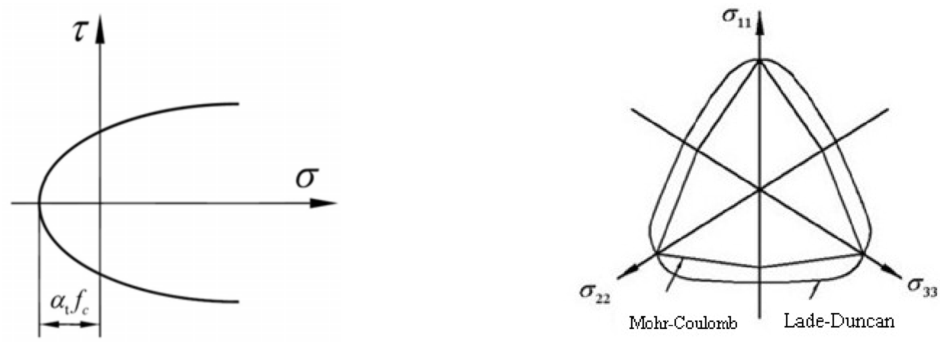

Fig. 1 Projections of improved Lade-Duncan failure criterion on meridian and π plane

$$g(\theta_\sigma)=\frac{1}{\sin(\frac{\pi}{3}+\frac{1}{3}\sin^{-1}(B\sin3\theta_\sigma))},-\frac{\pi}{6}\leq\theta_\sigma\leq\frac{\pi}{6} \tag{9}$$

making $k = g(\text{-}30°) / g(30°)$, the shear stress ratio k on the π plane is written as

$$k=\sqrt{\frac{J_{2c}}{J_{2e}}}=\frac{g(-\frac{\pi}{6})}{g(\frac{\pi}{6})}=\frac{\sin(\frac{\pi}{3}+\frac{1}{3}\sin^{-1}B)}{\sin(\frac{\pi}{3}-\frac{1}{3}\sin^{-1}B)} \tag{10}$$

2.2 Extended Lade-Duncan failure criterion

Based on research done by Hashiguchi (2002), an alternative form of Lade-Duncan failure criterion is proposed as

$$\frac{I_1^3}{I_3}=k_1=12+8\frac{1-\sin\phi_c}{1+\sin\phi_c}+6\frac{1+\sin\phi_c}{1-\sin\phi_c}+(\frac{1+\sin\phi_c}{1-\sin\phi_c})^2 \tag{11}$$

where φ_c is the frictional angle at the triaxial compression state.

According to the Mohr-Coulomb failure criterion, the ratio k on the π plane can be written as

$$k=\frac{3+\sin\phi_c}{3-\sin\phi_c} \tag{12}$$

Rearranging Eq. (12), then $\sin\varphi_c$ is expressed as

$$\sin\phi_c=3\frac{k-1}{k+1} \tag{13}$$

k is a function of I_1 and meets its boundary value condition k = 1~2, so its the simplest functional form should be proposed as

$$k=1+e^{-\eta I_1/f_c} \tag{14}$$

in which η is a material parameter and f_c is uniaxial compression strength of rock material.

Substituting Eq. (14) into Eq. (13) produces

$$\sin\phi_c = \frac{3e^{-\eta I_1/f_c}}{2+e^{-\eta I_1/f_c}} \tag{15}$$

Substituting Eq. (15) into Eq. (11), Eq. (11) is further expanded as

$$\frac{I_1^3}{I_3} = k_1 = 12 + 8\frac{1-\dfrac{3e^{-\eta I_1/f_c}}{2+e^{-\eta I_1/f_c}}}{1+\dfrac{3e^{-\eta I_1/f_c}}{2+e^{-\eta I_1/f_c}}} + 6\frac{1+\dfrac{3e^{-\eta I_1/f_c}}{2+e^{-\eta I_1/f_c}}}{1-\dfrac{3e^{-\eta I_1/f_c}}{2+e^{-\eta I_1/f_c}}} + \left(\frac{1+\dfrac{3e^{-\eta I_1/f_c}}{2+e^{-\eta I_1/f_c}}}{1-\dfrac{3e^{-\eta I_1/f_c}}{2+e^{-\eta I_1/f_c}}}\right)^2 \tag{16}$$

On the other hand, for more general geomaterials with the cohesion c and the tensile strength, in order to include the contribution of the cohesion and the tensile strength in the failure criterion, a translation of the principal stress space along the hydrostatic axis should be performed (Lade 1982, Houlsby 1986). Thus a stress item is added to the normal stress as follows

$$\begin{aligned}\overline{\sigma}_{11} &= \sigma_{11} + \alpha_t \cdot f_c \\ \overline{\sigma}_{22} &= \sigma_{22} + \alpha_t \cdot f_c \\ \overline{\sigma}_{33} &= \sigma_{33} + \alpha_t \cdot f_c\end{aligned} \tag{17}$$

in which α_t is a material parameter. The value of $\alpha_t \cdot f_c$ reflects the effect of the tensile strength σ_t of geomaterials.

Therefore, for more general geomaterials with cohesion c and tensile strength, a more general Lade-Duncan failure criterion is expressed as

$$\frac{\overline{I}_1^3}{\overline{I}_3} = \overline{k}_1 = 12 + 8\frac{1-\dfrac{3e^{-\eta \overline{I}_1/f_c}}{2+e^{-\eta \overline{I}_1/f_c}}}{1+\dfrac{3e^{-\eta \overline{I}_1/f_c}}{2+e^{-\eta \overline{I}_1/f_c}}} + 6\frac{1+\dfrac{3e^{-\eta \overline{I}_1/f_c}}{2+e^{-\eta \overline{I}_1/f_c}}}{1-\dfrac{3e^{-\eta \overline{I}_1/f_c}}{2+e^{-\eta \overline{I}_1/f_c}}} + \left(\frac{1+\dfrac{3e^{-\eta \overline{I}_1/f_c}}{2+e^{-\eta \overline{I}_1/f_c}}}{1-\dfrac{3e^{-\eta \overline{I}_1/f_c}}{2+e^{-\eta \overline{I}_1/f_c}}}\right)^2 \tag{18}$$

where the first and third stress tensor invariants $\overline{I}_1$ and $\overline{I}_3$ could be calculated based on the new stress tensors $\overline{\sigma}_{11}$, $\overline{\sigma}_{22}$ and $\overline{\sigma}_{33}$, separately.

Similar to the solution of Eq. (7), an alternative form of the Eq. (18) is obtained as

$$\sqrt{J_2} = \frac{\overline{B}\overline{I}_1}{2\sqrt{3}}\overline{g}(\theta_\sigma) \tag{19}$$

in which $\overline{B}$ and $\overline{g}(\theta_\sigma)$ are formulated as

$$\overline{B} = \sqrt{\frac{\overline{k}_1 - 27}{\overline{k}_1}} \tag{20}$$

$$\overline{g}(\theta_\sigma) = \frac{1}{\sin\left(\dfrac{\pi}{3} + \dfrac{1}{3}\sin^{-1}(\overline{B}\sin 3\theta_\sigma)\right)}, -\frac{\pi}{6} \le \theta_\sigma \le \frac{\pi}{6} \tag{21}$$

Therefore, the more general Lade-Duncan failure criterion containing two unknown material parameters η and α_t, could describe strength characteristics of geomaterials such as friction, tensile strength or cohesion, and curved meridian in the three-dimensional principal stress space. The Eqs. (18) and (19) are further explained by Fig. 1(a) in the meridian plane and by Fig. 1(b) in the π plane, separately. The Eq. (18) was further verified to be reasonable for predicting strengths of rock materials by Yang *et al.* (2006a).

3. Failure criterion of transversely isotropic rock materials

3.1 Fabric tensor

Shale is a widespread sedimentary rock containing obviously visible bedding structures, which can be described by material fabric tensor F_{ij}. It can be proved that the F_{ij} is symmetric, and therefore, it can always be described by three material principal values, such as F_{11}, F_{22} and F_{33}. If the reference frame is coincident with the material principal axes, then the fabric tensor can be written as

$$F'_{ij} = \begin{pmatrix} F_{11} & 0 & 0 \\ 0 & F_{22} & 0 \\ 0 & 0 & F_{33} \end{pmatrix} \tag{22}$$

In most cases, rock material is transversely isotropic, which means that two of the principal values, say, F_{22} and F_{33}, are equal. The F_{ij} possesses a unit trace, thus F_{11} = 1-2F_{33}. Oda and Nakayama (1989) showed that the fabric tensor for such material can be written in the following form:

$$F'_{ij} = \frac{1}{3+\Delta}\begin{pmatrix} 1-\Delta & 0 & 0 \\ 0 & 1+\Delta & 0 \\ 0 & 0 & 1+\Delta \end{pmatrix} \tag{23}$$

where Δ = a measurable quantity called the vector magnitude, which indicates the magnitude of the anisotropy of the preferred orientation of the particles. $\Delta = 0$ corresponds to a fabric formation isotropically, $\Delta = 1$ implies a fabric formation in which major axes of all the particles are uniformly distributed in the horizontal bedding plane.

Note that if the sample has rotated, and /or the reference frame has changed, the components of the fabric tensor F_{ij} will be subjected to an orthogonal transformation as follows

$$F_{ij} = Q_{ki}Q_{lj}F'_{kl} \tag{24}$$

where $Q_{ij} = e'_i \cdot e_j$ is the cosine of the angle between e'_i, the ith base vector in the original frame, and e_j, the j^{th} base vector in the new reference frame. In general, the off-diagonal components of F_{ij} do not vanish.

3.2 The anisotropic state parameter

Recalling the definition of the intermediate principal stress ratio $b = (\sigma_{22} - \sigma_{33}) / (\sigma_{11} - \sigma_{33})$ in terms of the three principal stresses, one can write $\sigma_{22} = b\,\sigma_{11} + (1\text{-}b)\,\sigma_{33}$ and $p = \sigma_{ij} / 3 = [(1+b)\,\sigma_{11} + (2–b)\,\sigma_{33}]$, then further define ***s*** and subsequently the unit deviatoric tensor $n_{ij} = s_{ij} / |s|$ in terms of b. Then the following expression for the components n_{ij} of ***n*** is written as

$$[n] = \frac{1}{\left[6(b^2 - b + 1)\right]^{1/2}} \begin{bmatrix} 2-b & 0 & 0 \\ 0 & 2b-1 & 0 \\ 0 & 0 & -(1+b) \end{bmatrix} \tag{25}$$

Based on Eq. (25), the unit deviatoric tensor ***n*** satisfying Tr***n*** = 0, and Tr$\boldsymbol{n}^2$ = 1(Tr = trace), therefore, presents the direction of the deviatoric stress tensor in principal stress space, and does not contain the deviatoric stress tensor amplitude. Furthermore, the result of ***F:n*** can be considered as a physically motivated measure of interaction of the fabric tensor and stress tensor, portrayed by ***F*** and ***n***, respectively. Because Tr***n*** = 0, the ***F:n*** further reflects the interaction of the deviatoric fabric tensor and the unit deviatoric stress tensor in nature. Similar to the definition proposed by Dafalias *et al.* (2004) with a small difference, the anisotropic state parameter A in this paper is directly expressed in the following form

$$A = F_{ij} n_{ij} = F_{ij}^{\pi} n_{ij} \tag{26}$$

in which $F_{ij}^{\pi} = F_{ij} - F_{kk}\delta_{ij} / 3$.

3.2.1 Torsional shear tests

For the torsional shear tests shown in Fig. 2, the F_{ij} are given by Eq. (24), while in reference to the axes of σ_1, σ_2 and σ_3, the n_{ij} are given by Eq. (25). This enables the calculation of the anisotropic state parameter A from Eq. (26) written as

$$A = \sqrt{\frac{2}{3}} \cdot \frac{\Delta}{3+\Delta} \cdot \frac{1}{(b^2 - b + 1)^{1/2}} (1 + b - 3\cos^2\alpha) = \frac{D}{(b^2 - b + 1)^{1/2}} (1 + b - 3\cos^2\alpha) \tag{27}$$

in which $D = \sqrt{2/3}\Delta/(3+\Delta)$. It can be seen that the anisotropic state parameter A is a function containing the variables Δ, b and a. Fig. 3 gives variation of the anisotropic state parameter A against angle a at different b values and at a given $D = 0.0447$.

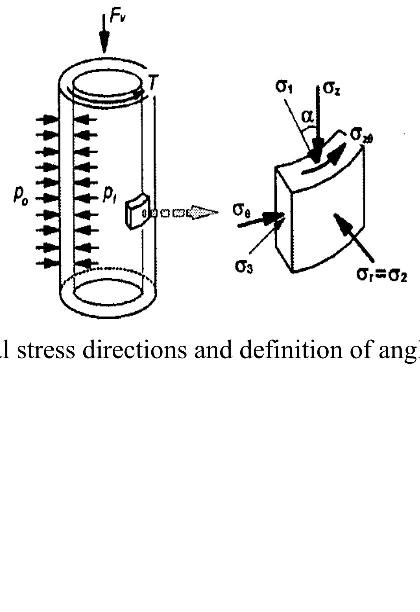

Fig. 2 Rotation of principal stress directions and definition of angle a in torsional shear tests

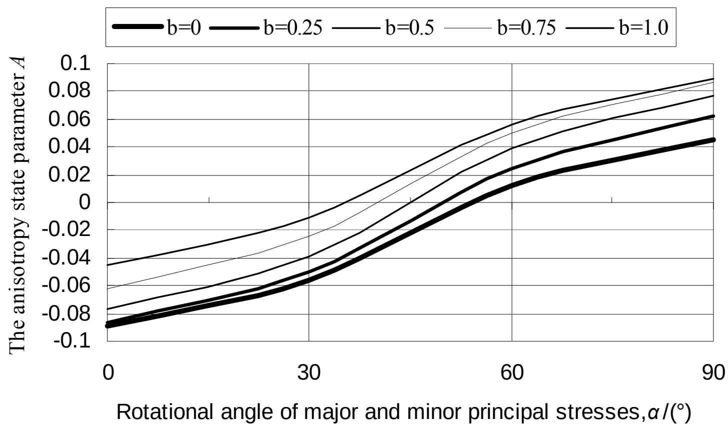

Fig. 3 Variation of the anisotropic state parameter A against angle a at different b values (D = 0.0447)

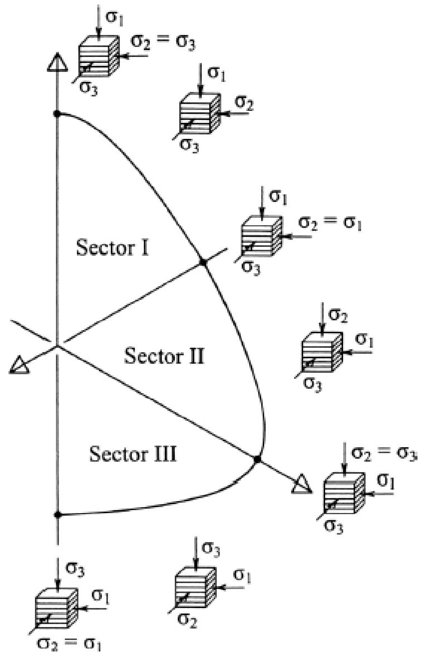

Fig. 4 Application of major, intermediate and minor principal stresses to specimen with bedding planes in true triaxial tests (after Lade (2008))

Under rock uniaxial compressive state, with b = 0 at the state, the anisotropic state parameter A in Eq. (27) is further simplified as

$$A = D(1 - 3\cos^2 \alpha) \tag{28}$$

3.2.2 True triaxial tests

For true triaxial tests, the b value varies from b = 0 at triaxial compression to b = 1 at triaxial extension in each of the three sectors, as shown on the octahedral plane in Fig. 4. In this figure the major, intermediate and minor principal stresses are indicated as σ_1, σ_2 and σ_3 respectively, and further shown in orientation relative to the bedding planes of the samples for each of the three sectors.

(1) Sector I

As shown in Fig. 4, the anisotropic state parameter A in sector I based on Eq. (27) is expressed by

$$A = F_{ij}n_{ij} = \sqrt{\frac{2}{3}} \cdot \frac{\Delta}{3+\Delta} \cdot \frac{b-2}{(b^2-b+1)^{1/2}} \tag{29}$$

At triaxial compression, $b = 0$, $A = -2D$. At triaxial extension, $b = 1$, $A = -D$.

(2) Sector II

Shown in Fig. 4, the anisotropic state parameter A in sector II based on Eq. (26) is written as

$$A = F_{ij}n_{ij} = \sqrt{\frac{2}{3}} \cdot \frac{\Delta}{3+\Delta} \cdot \frac{1-2b}{(b^2-b+1)^{1/2}} \tag{30}$$

At triaxial compressio, $b = 0$, $A = D$. At triaxial extension, $b = 1$, $A = -D$.

(3) Sector III

As shown in Fig. 4, the anisotropic state parameter A in sector III based on Eq. (27) is expressed as

$$A = F_{ij}n_{ij} = \sqrt{\frac{2}{3}} \cdot \frac{\Delta}{3+\Delta} \cdot \frac{1+b}{(b^2-b+1)^{1/2}} \tag{31}$$

At triaxial compression, $b = 0$, $A = D$. At triaxial extension, $b = 1$, $A = 2D$.

It should be noted that the relative orientation of stress tensor and fabric tensor in sector I in Fig. 4 is equivalent to the relative orientation of stress tensor and fabric tensor for the torsional shear tests with $a = 0°$ shown in Fig. 2. The anisotropic state parameters at $b = 0$ in sector I and at $b = 0$ with $\alpha = 0°$ for the torsional shear tests are both equal to the same value $A = -2D$.

The relative orientation of stress and fabric tensors in sector III in Fig. 4 is equivalent to the relative orientation of stress and fabric tensors for the torsional shear tests with $a = 90°$ shown in Fig. 2. The anisotropic state parameters at $b = 1$ in sector III and at $b = 1$ with $a = 90°$ for the torsional shear tests are both equal to the same value $A = 2$.

3.3 Failure criterion of transversely isotropic rock materials

Following the framework developed in Pietruszczak *et al.* (2001, 2002), and based on definition of the anisotropic state parameter A, assume that the failure criterion of transversely isotropic rock materials can be expressed in a simplified form

$$f = f(\sigma_{ij}, F_{ij}) = f(I_1, J_2, J_3, A) \tag{32}$$

For an isotropic rock material with $A = 0$, the corresponding failure criterion is expressed by Eq. (18). For transversely isotropic rock material with $A \neq 0$, the corresponding failure criterion can be developed by the Eq. (18) incorporating an anisotropic state scalar parameter. In order to account for inherent anisotropy, assume that f_c is affected by the orientation of the sample with its stress tensor, and its variation is described by incorporating a distribution function as

$$f_c = \hat{f}(1 + F_{ij}n_{ij} + F_{ijkl}n_{ijkl} + F_{ijklmn}n_{ijklmn} + \cdots) \tag{33}$$

A special case of the representation corresponds to introducing the following expression as $F_{ijkl}n_{ijkl} = d_1 F_{ij}F_{kl}n_{ij}n_{kl}$, $F_{ijklmn}n_{ijklmn} = d_2 F_{ij}F_{kl}F_{mn}n_{ij}n_{kl}n_{mn}$, etc. Further, Eq. (33) is expanded as

$$\begin{aligned} f_c &= \hat{f}[1 + F_{ij}n_{ij} + d_1(F_{ij}n_{ij})^2 + d_2(F_{ij}n_{ij})^3 + d_3(F_{ij}n_{ij})^4 + \cdots] \\ &= \hat{f}[1 + A + d_1A^2 + d_2A^3 + d_3A^4 + \cdots] \\ &= \hat{f}\left\{1 + D(1-3\cos^2\alpha) + d_1[D(1-3\cos^2\alpha)]^2 + d_2[D(1-3\cos^2\alpha)]^3 + d_3[D(1-3\cos^2\alpha)]^4 + \cdots\right\} \end{aligned} \tag{34}$$

In Eq. (34), $\hat{f}$, d_1, d_2, d_3,… are constants to be identified further.

Then, the failure criterion of the transversely isotropic rock material is easily obtained through replacing f_c of Eq. (34) into Eq. (18).

4. Parameter determination

4.1 Parameter determination for Eq. (34)

Consider first Eq. (34), which describes the variation of the uniaxial compressive strength f_c. The relevant experimental data is provided by Niandou *et al.* (1997) in Fig. 5, which shows the variation of f_c with the orientation of bedding planes measured in terms of the angle α.

If item $A = F_{ij}n_{ij}$ of degree up to 1 is kept, the Eq. (34) is further simplified as

$$f_c = \hat{f}[1 + D(1-3\cos^2\alpha)] \tag{35}$$

Based on Eq. (35) combined with uniaxial compressive strength testing data of Tournemire shale, then $\hat{f} = 28.46\,\text{MPa}$ and $D = 1$ can be obtained through the best fitting technique.

If item $A = F_{ij}n_{ij}$ of degree up to 2 is kept, the Eq. (34) is simplified as

$$f_c = \hat{f}\left\{1 + D(1-3\cos^2\alpha) + d_1[D(1-3\cos^2\alpha)]^2\right\} \tag{36}$$

Based on Eq. (36) combined with uniaxial compressive strength testing data, then $\hat{f} = 20.36\,\text{MPa}$, $D = 0.31583$ and $d_1 = 4.1816$ can be obtained through the best fitting technique.

If item $A = F_{ij}n_{ij}$ of degree up to 4 is used, the Eq. (34) is simplified as

$$f_c = \hat{f}\left\{1 + D(1-3\cos^2\alpha) + d_1[D(1-3\cos^2\alpha)]^2 + d_2[D(1-3\cos^2\alpha)]^3 + d_3[D(1-3\cos^2\alpha)]^4\right\} \tag{37}$$

Based on Eq. (37) combined with the uniaxial compressive strength testing data, then $\hat{f} = 22.56\,\text{MPa}$, $D = 0.0447$, $d_1 = 51.831$, $d_2 = 2949.6912$ and $d_3 = 42962.887$ can be obtained

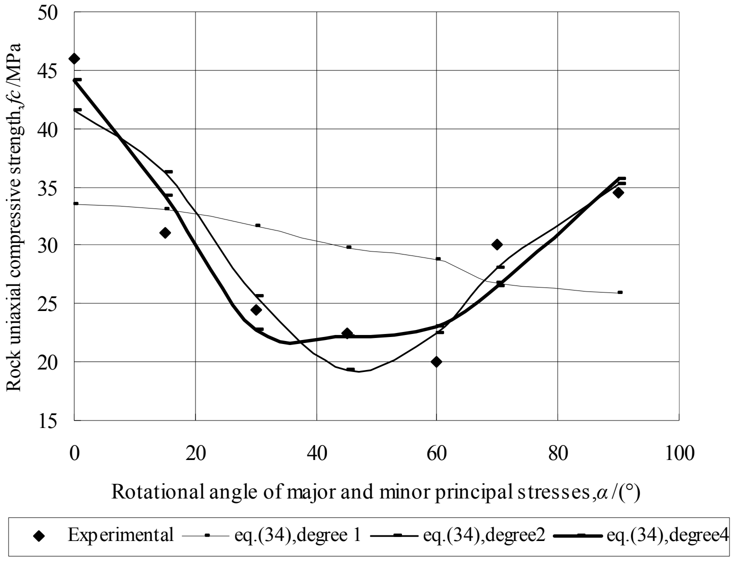

Fig. 5 Testing uniaxial compressive strengths of Tournemire shale with its theoretical predicting results

through the best fitting technique.

Comparisons of the rock uniaxial compressive strengths with the theoretical predictions, which are calculated by Eqs. (35), (36) and (37) respectively, are shown in Fig.5. It is shown from the figure that Eq. (37) containing item $A = F_{ij}n_{ij}$ with degree up to 4, giving the best fitting for the results, thus can be applied to the transversely isotropic rock material with obviously fabric difference between F_{11} and F_{33}. On the other hand, Eq. (35) containing term $A = F_{ij}n_{ij}$ of degree up to 1 predicting f_c as a gently decreasing value as the angle α increases, thus can be applied to structured soils with relative weakly fabric difference between F_{11} and F_{33}.

4.2 Parameters in failure criterion

4.2.1 Parameter α_t

Based on the test data of the Tournemire shale provided by Niandou *et al.* (1997), both the uniaxial compressive strength f_c = 46 MPa for α = 0° and the triaxial tensile strength σ_t = 4.6 MPa are given. Therefore, the calculated value of $\alpha_t = \sigma_t / f_c = 0.1$.

4.2.2 Parameter η

Rearranging Eq. (15) produces

$$e^{-\eta \bar{I}_1 / f_c} = \frac{2\sin\phi_c}{3-\sin\phi_c} \tag{38}$$

Then material parameter η based on Eq. (38) is expressed as

$$\eta = \frac{\ln(3-\sin\phi_c) - \ln(2\sin\phi_c)}{\bar{I}_1 / f_c} \tag{39}$$

sin ϕ_c in Eq. (39) can be given based on the Tournemire shale conventional triaxial compressive data (σ_{11}, $\sigma_{22} = \sigma_{33}$), expressed as

$$\sin\phi_c = \frac{(\bar{\sigma}_{11} - \bar{\sigma}_{33})/f_c}{(\bar{\sigma}_{11} + \bar{\sigma}_{33})/f_c} = \frac{(\sigma_{11} - \sigma_{33})/f_c}{(\sigma_{11} + \sigma_{33})/f_c + 2\alpha_t} \tag{40}$$

Therefore, based on the n set triaxial compressive failure data (σ_{11}, $\sigma_{22} = \sigma_{33}$) of the Tournemire shale, n set sin ϕ_c values can be calculated based on Eq. (40), and n set η values can be obtained further based on Eq. (39). In a larger range of applied confinement stresses such as $\sigma_{33} = 0 \sim 50$ MPa, η will change as the stress level $\bar{I}_1 / f_c$ changes. In order to correctly simulate the strength curve in the meridian plane, η should be further adjusted as

$$\eta = \eta_0 + \eta_1 \bar{I}_1/f_c + \eta_2(\bar{I}_1/f_c)^2 \tag{41}$$

Combining the η values given by the above Eq. (39), the parameters $\eta_0 = 0.22702$, $\eta_1 = -1.7453 \times 10^{-2}$ and $\eta_2 = 4.5601 \times 10^{-4}$ in Eq. (41) can be obtained through the best fitting technique.

5. Verification

5.1 Verification by torsional shear tests

Putting f_c of Eq. (37) into Eq. (18), then failure criterion of transversely isotropic rock material is obtained. By using the new failure criterion with the above identified parameters, theoretical prediction curves of $\sqrt{J_2} \sim \alpha$ with $b = 0$ being plotted for the Tournemire shale, under different σ_{33} stress levels, are compared with the experimental rock triaxial shear strengths as shown in Fig. 6.

Based on the new failure criterion with $b = 0.25, 0.5, 0.75, 1.0$ respectively, additional relations of $\sqrt{J_2} \sim \alpha$ for the Tournemire shale are predicted for different σ_{33} stress levels, as disclosed in Fig. 7.

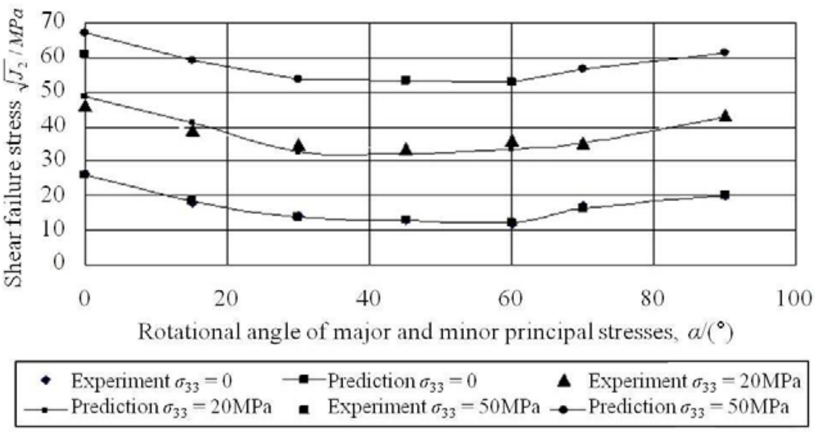

Fig. 6 Testing triaxial shear strengths of Tournemire shale with its theoretical predictions for $b = 0$

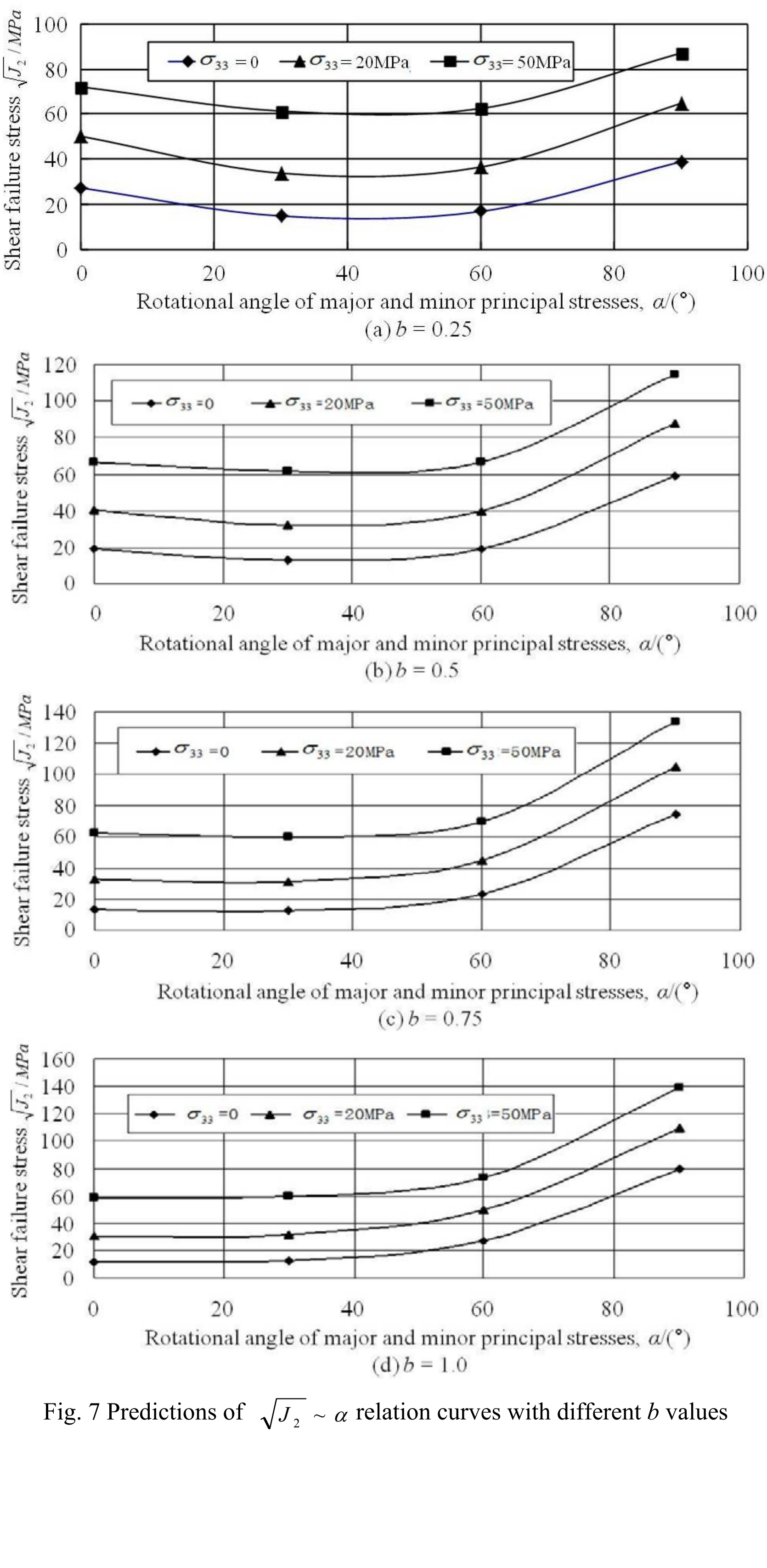

Fig. 7 Predictions of $\sqrt{J_2} \sim \alpha$ relation curves with different b values

Based on Fig. 6, the new failure criterion, i.e., the improved Eq. (18), can give reasonable prediction results of the strength of Tournemire shale. The main reason should be due to the normalized quantify $[\eta \cdot \bar{I}_1 / f_c(\alpha)]$ in Eq. (18), by which the anisotropy of the transversely isotropic Tournemire shale, depending on the interaction of the fabric tensor and the unit deviatoric stress tensor, is gotten rid of naturally.

Under the torsional shear mode shown in Fig. 2, some 10.5 m bgl (below ground level) natural London Clays are anisotropically consolidated (AC) and other 10.5m bgl natural London Clays are isotropically consolidated (IC) before shearing, respectively. The peak stress ratios, q/p, observed for b = 0.5, are plotted in Fig. 8(a) against the α values applied at failure for the 10.5 m bgl natural London clays. Fig. 8 (b) shows the anisotropy of the undrained shear strength S_u. The shear strength anisotropy is clearly recognizable in these cases. Comparison of the Fig. 7(b) with the Fig. 8 shows that for the Tournemire shale and the natural London Clays, their peak shear strengths both have the same tendency for change against the α values.

It is of interest to compare the anisotropy of the natural London Clays (with OCR>9) with the more familiar patterns known for low-OCR reconstituted soils. Fig. 9 shows the S_u anisotropy of

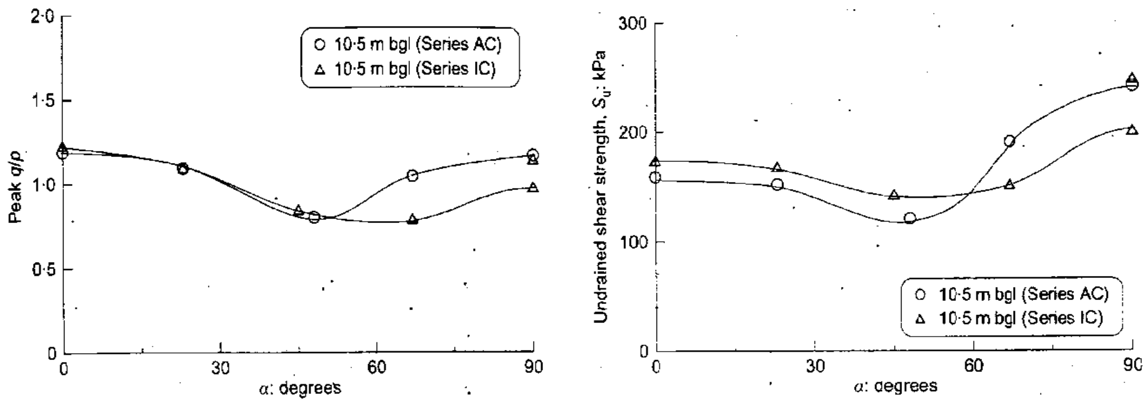

(a) (b)

Fig. 8 Variation tendency of peak shear strength of natural London Clay as α being changed with b = 0.5 (after Nishimura (2007))

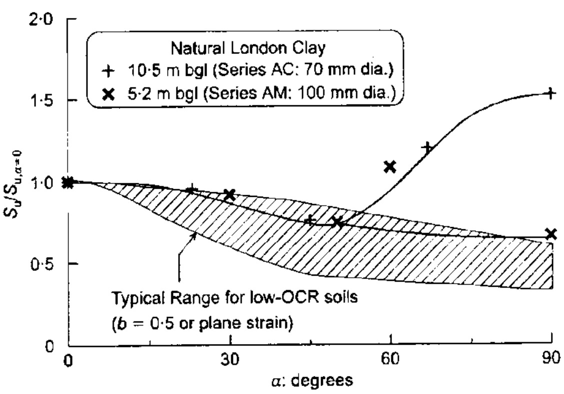

Fig. 9 Undrained shear strength anisotropy of low-OCR k_0-reconstituted soils and natural London Clay (after Nishimura(2007))

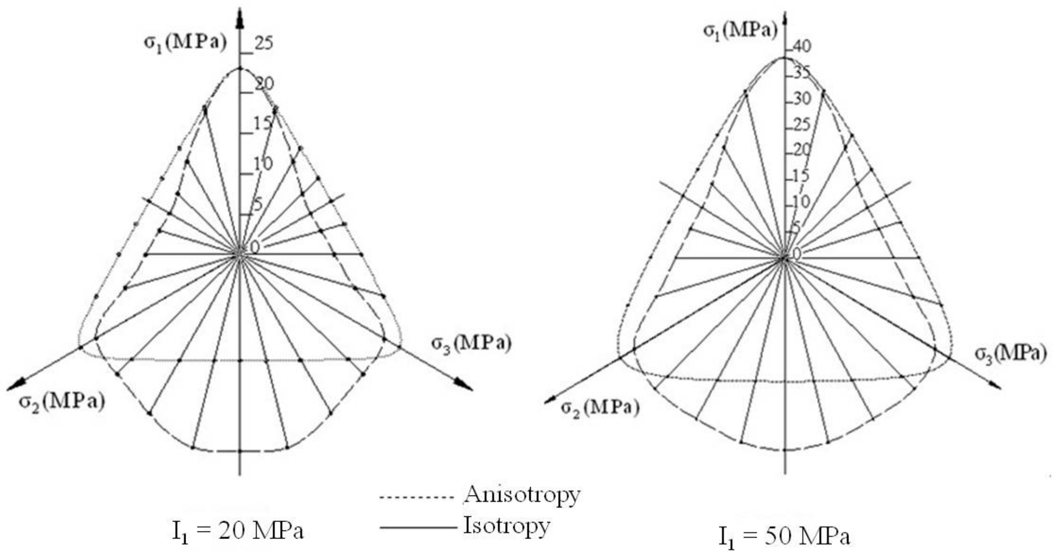

Fig. 10 Failure envelopes of Tournemire shale in I, II and III sectors on corresponding π planes

the natural London Clay for b = 0.5, normalized by the S_u at α = 0°. The shaded area indicates the range of results from previously published tests on low-OCR (OCR = 1~4) k_0- reconstituted soils including clay, silt, and clayey and silty soils. The low-OCR soils generally exhibit S_u falling monotonically against α values, giving $S_{u,\alpha=90°}$ / $S_{u,\alpha=0°=0.3\sim0.6}$, which was shown by Lade (1990), and Whittle *et al.* (1994). However, the upper data curve for the London Clay obtained from AC, follows the opposite trend with the $S_{u,\alpha=90°}$ / $S_{u,\alpha=0°}$ ratio being as high as 1.5. Whereas this upper data curve is considered to reflect the influence of both the micro- and the macro- fabric, the lower data curve obtained from 5.2 m bgl may further reflect the discontinuous, high fissured macrofabric. Heavily overconsolidated London Clay (with OCR > 9) appears to change the microstructural anisotropy from that seen at low OCR, while discontinuities developed, most probably during or after the overconsolidation, modify the anisotropy further.

If the microstructural fabric of Tournemire shale is similar to that of the heavily overconsolidated the London Clay, this may provide a reasonable explanation regarding the peak shear strength variation against the α in Fig. 7(b) being approximately the same as that of the London Clay shown in Fig. 8.

5.2 Verification by true triaxial tests

For true triaxial tests, substitution of Eqs. (29), (30) and (31) into Eq. (34) respectively, then different formulation of f_c, in sectors I, II and III, is expressed as follows

$$\text{I:}\quad f_c=\hat{f}\left\{1+D\cdot\frac{b-2}{(b^2-b+1)^{1/2}}+d_1[D\cdot\frac{b-2}{(b^2-b+1)^{1/2}}]^2+d_2[D\cdot\frac{b-2}{(b^2-b+1)^{1/2}}]^3+d_3[D\cdot\frac{b-2}{(b^2-b+1)^{1/2}}]^4\right\} \quad (42a)$$

$$\text{II:}\quad f_c=\hat{f}\left\{1+D\cdot\frac{1\text{-}2b}{(b^2-b+1)^{1/2}}+d_1[D\cdot\frac{1\text{-}2b}{(b^2-b+1)^{1/2}}]^2+d_2[D\cdot\frac{1\text{-}2b}{(b^2-b+1)^{1/2}}]^3+d_3[D\cdot\frac{1\text{-}2b}{(b^2-b+1)^{1/2}}]^4\right\} \quad (42b)$$

$$\text{III:} \quad f_c = \hat{f}\left\{1 + D\cdot\frac{1+b}{(b^2-b+1)^{1/2}} + d_1[D\cdot\frac{1+b}{(b^2-b+1)^{1/2}}]^2 + d_2[D\cdot\frac{1+b}{(b^2-b+1)^{1/2}}]^3 + d_3[D\cdot\frac{1+b}{(b^2-b+1)^{1/2}}]^4\right\} \tag{42c}$$

Substitution of Eq. (42) into the Eq. (18) and combined with the given parameters identified above, the failure envelopes of the Tournemire shale calculated by the improved Eq. (18) in sectors I, II and III on π planes with different stress levels, are plotted in Fig. 10.

From Fig. 10, it is seen that the Tournemire shale has obviously transverse anisotropy at lower stress levels, and the anisotropy is further constrained as the stress level is increased, which makes the Tournemire shale develop toward the state of a homogeneous media.

6. Conclusions

(1) For rock materials, a transversely isotropic failure criterion, established through the extended Lade-Duncan failure criterion incorporating an anisotropic state scalar parameter, which is a joint invariant of deviatoric microstructure fabric tensor and normalized deviatoric stress tensor, is proposed in this paper. The theoretically predicted results being consistent with the Tournemire shale test data at peak failure shown in Fig. 6 indicates that the transversely isotropic failure criterion is reasonable.

(2) For the torsion shear mode with $0 \le b \le 0.75$, the rock shear strength decreases with α increasing until the rock shear strength approaches a minimum value at $\alpha \approx 40°$, and after the minimum value, the rock shear strength increases as α increases further. For the torsion shear mode with $b > 0.75$, the rock shear strength is almost kept constant when $\alpha \le 40°$, and after that, the rock shear strength increases as α increases further. The rock shear strength tendency against α agrees with the shear strength variation against α of the heavily OCR natural London Clays tested before.

(3) From Fig. 10, it is seen that the strength anisotropy of the Tournemire shale is further suppressed as σ_{33} being increased continuously, which makes the Tournemire shale develop toward the state of a homogeneous media. This phenomenon coincides our engineering experiences.

(4) Parameter η of Eq. (41) being a polynomial function of $\bar{I}_1/f_c$ can be treated flexibly according to the stress range such that when the confinement stress variation range is larger, we can choose the item $\bar{I}_1/f_c$ with degree up to 2 or higher value to obtain the correct Eq. (41) to describe the variable parameter η. When confinement stress variation range is narrow, we can choose the item $\bar{I}_1/f_c$ of degree up to 1 or even null to simulate rock material failure correctly.

Acknowledgements

Authors hope to express their many thanks to Prof. P.V. Lade, Dr. Hamid Karimpour and Ms Lilian Ndongmo for revising this paper.

References

Dafalias, Y.F., Papadimitriou, A.G. and Li, X.S. (2004), “Sand plasticity model accounting for inherent fabric anisotropy”, *J. Eng. Mech*., **130**(11), 1319-1333.
Hashiguchi, K. (2002), “A proposal of the simplest convex-conical surface for soils”, *Soil. Found*., **42**(3), 107-113.
Houlsby, G.T. (1986), “A general failure criterion for frictional and cohesive materials”, *Soil. Found*., **26**(2), 97-101.
Lade, P.V. and Duncan, J.M. (1975), “Elastoplastic stress-strain theory for cohesionless soil”, *J. Geotech. Eng. - ASCE*, **101**(10), 1037-1053.
Lade, P.V. (1982), “Three –parameter failure criterion for concrete”, *J. Eng. Mech. Div. - ASCE*, **108**(5), 850-563.
Lade, P.V. (1990), “Single-hardening model with application to NC clay”, *J. Geotech. Eng*., **116**(3), 394-414.
Lade, P.V. (2008), “Failure criterion for cross-anisotropic soils”, *J. Geotech. Geoenviron. Eng*., **124**(1), 117-124.
Li, X.S. and Dafalias, Y.F. (2002), “Constitutive modeling of inherently anisotropic sand behavior”, *J. Geotech. Geoenviron. Eng.*, **128**(10), 868-880.
Niandou, H., Shao, J.F. and Henry, J.P. *et al*. (1997), “Laboratory investigation of the mechanical behavior of Tournemire shale”, *Int. J. Rock. Mech. Min. Sci*., **34**(1), 3-16.
Nishimura, S., Minh, N.A. and Jardine, R.J. (2007), “Shear strength anisotropy of natural London clay”, *Geotechnique*, **57**(1), 49-62.
Ochiai, H. and Lade, P.V. (1983), “Three-dimensional behavior of sand with anisotropic fabric”, *J. Geotech. Eng*., **109**(10), 1313-1328.
Oda, M. (9172), “Initial fabrics and their relations to mechanical properties of granular materials”, *Soil. Found*., **12** (1), 17-36.
Oda, M. and Nayayama, H. (1989), “Yield function for soil with anisotropic fabric”, *Eng. Mech. - ASCE*, **115**(1), 89-104.
Pietruszczak, S. and Mroz, Z. (2001), “On failure criteria for anisotropic cohesive-frictional materials”, *Int. J. Numer. Anal. Method. Geomech.*, **25**(5), 509-524.
Pietruszczak, S., Lydzba, D. and Shao, J.F. (2002), “Modeling of inherent anisotropy in sedimentary rock”. *Int. J. Solid. Struct*., **39**, 637-648.
Yang, X.Q., Fung, W.H. and Au, S.K. *et al*. (2006a), “A note on the Lade-Duncan failure criterion”, *Geomech. Geoeng. Int. J.*, **1**(4), 299-304.
Yang, X.Q., Zhu, Z.Z. and He, S.X. *et al*. (2006b), “Researches on failure criteria of Lade-Duncan, Matsuoka-Nakai and Ottosen”, *Chinese J. Geotech. Eng*., **28**(3), 337-342. (in Chinese)
Whittle, A.J., DeGroot, D.J. and Ladd, C.C. *et al*. (1994), “Model prediction of anisotropic behavior of Boston Blue clay”, *J. Geotech. Eng*., **120**(1), 199-224.

PL